ISSN print: 1224-5984
ISSN online: 2248-3942

Rom Biotechnol Lett. 2022; 27(3): 3507-3516
doi: 10.25083/rbl/27.3/3507.3516

Received for publication: July, 20, 2022
Accepted: August 11, 2022

Original paper

PETase from *Ideonella sakaiensis*: towards facile bacterial expression system

KRISZTINA BOROS[1], ILKA HORVÁTH[1], CĂTĂLINA ROTARU[1], RALUCA BIANCA TOMOIAGĂ[1], DR. MONICA IOANA TOŞA[1], DR. LÁSZLÓ-CSABA BENCZE[1]*

[1]Enzymology and Applied Biocatalysis Research Center, Faculty of Chemistry and Chemical Engineering, Babeș-Bolyai University, Arany János Street 11, RO-400028 Cluj-Napoca, Romania

Abstract

One of the most promising PET-hydrolysing enzyme, *Is*PETase, originates from 'plastic-consuming' bacteria *Ideonella sakaiensis* and operates at moderate temperatures (30-40 °C) in aqueous environment, showing far higher hydrolysing efficiency than several cutinases. Accordingly, the development of proper recombinant expression system providing facile access to the isolated/purified *Is*PETase is also of high interest. In our aim to produce active recombinant *Is*PETase, the unsuccessful expression registered by employing several reported expression systems, directed us towards the optimization/development of a facile/accessible recombinant expression system suitable for *Is*PETase production. Testing several plasmid constructs, providing different N- or C-terminal affinity tags for the expression of full-length or truncated (residues 28-290) *Is*PETase and various *E. coli* expression hosts, revealed several non-reported issues hindering the recombinant expression of *Is*PETase. After optimization of the construct and expression host, the use of N-terminal His-tag and Rosetta-gami B expression host provided recombinant *Is*PETase in high purity and titer-yield. The thermal denaturation profile and PET-hydrolysing activity of the obtained *Is*PETase agree with the reported data, supporting proper folding of the purified protein. The results support that the *in vivo* folding process of *Is*PETase might be differently affected among the different *E. coli* host strains, moreover, underline the importance of the proper selection of the cloning strategy for the successful expression of the *Is*PETase.

Keywords Polyethylene terephthalate (PET), enzymatic PET degradation, *Is*PETase, protein expression

To cite this article: BOROS K, HORVÁTH I, ROTARU R, TOMOIAGĂ RB, TOŞA MI, BENCZE L. PETase from *Ideonella sakaiensis*: towards facile bacterial expression system. *Rom Biotechnol Lett.* 2022; 27(3): 3507-3516 DOI: 10.25083/rbl/27.3/3507.3516

*Corresponding author: Dr. László Csaba Bencze; email: laszlo.bencze@ubbcluj.ro

Introduction

Since several decades, polyethylene terephthalate (PET), the polymerization product of ethylene glycol (EG) and terephthalate (TPA), is one of the most produced and most widely used plastics in the world and thus accumulates in the environment at a staggering rate (W. COURTENE-JONES & al. [1]; L. NIZZETTO & al. [2]; C. E. ENYOH & al. [3]; C. L. WALLER & al. [4]; R. H. WARING & al. [5]; E. S. GRUBER & al. [6]; K. RAGAERTA & al. [7]). Plastic particles can be detected in both marine and terrestrial ecosystems, from surface waters to deep-sea sediments, on the shorelines of every continent, in soils and freshwater, even in the polar regions, but are also present in the air (W. COURTENE-JONES & al. [1]; L. NIZZETTO& al. [2]; C. E. ENYOH & al. [3]; C. L. WALLER & al. [4]). Moreover, plastic particles ingested by animals, enter the food chain and accumulate in the organisms (W. COURTENE-JONES & al. [1]; R. H. WARING & al. [5]), with more recent studies revealing their toxic effects (E. S. GRUBER & al. [6]), however their long-term biological effect mainly remains unexplored.

Recycling PET is one of the solutions for reducing plastic pollution, which is already taking place at various rates worldwide. However, the classic, thermomechanical PET recycling, leads to a loss of the polymer`s mechanical properties, while the chemical degradation/recycling requires harsh conditions, consumes large amount of energy and generates toxic secondary pollutants (K. RAGAERTA & al. [7]). In 2005, the possibility of enzymatic hydrolysis of PET films was firstly reported (R. J. MÜLLER & al. [8]), followed by further significant efforts to provide an industrially feasible and efficient, eco-friendly, biocatalytic PET degradation method (H. F. SON & al. (2020) [9]; H. P. AUSTIN & al. [10]; Y. MA & al. [11]; H. Y. SAGONG & al. [12]; R. WEI & al. [13]; F. KAWAI & al. (2019) [14]). One of the main obstacles remained the inaccessibility of the amorphous domains of the PET polymer for the enzymatic attack, due to the high glass transition temperature (around 75 °C) of PET, thus the biocatalytic degradation efficiency being affected by the different crystallinity degree among the different type of PET pollutants (R. WEI & al. [13]). In this context enzyme variants with improved stability under severe conditions, such as high temperature and presence of swelling agents, are highly desirable (F. KAWAI & al. (2019) [14]), reflecting current research directions in enzymatic PET degradation (F. KAWAI & al. (2020) [15]). Among the enzymes possessing PET-degrading activity, hydrolases such as cutinases (T. BRUECKNER & al. [16a]; E. H. ACERO & al. [16b]; F. KAWAI & al. (2017) [16c]), lipases (M. A. M. E. VERTOMMEN & al. [17]) and PETases (I. TANIGUCHI & al. [18]) have been reported. One of the most promising PET-hydrolysing enzyme, *Is*PETase, derives from 'plastic-consuming' bacteria *Ideonella sakaiensis* (S. YOSHIDA & al. [19]) and operates in aqueous environment with far higher PET-hydrolysing efficiency at moderate temperatures (30-40 °C) than cutinases from *Humicola insolens* (*Hi*C) and from *Thermobifida fusca* (*Tf*Cut1 and *Tf*Cut2), hydrolases from *Thermobifida fusca* (*Tjjf*H) or lipase from *Candida antarctica* (S. JOO & al. [20]; H. F. SON & al. (2019) [21]). Since, in order to carry out the PET-degradation, *Is*PETase needs to be secreted extracellularly or to be used as isolated enzyme biocatalyst, the development of proper recombinant expression system providing facile access to the isolated/purified *Is*PETase is also of high interest.

In our aim to produce active recombinant *Is*PETase and the unsuccessful set-up of several reported expression systems (H. F. SON & al. (2020) [9]; H. P. AUSTIN & al. [10]; S. JOO & al. [20]; H. F. SON & al. (2019) [21]; G. J. PALM & al. [22]; C. LIU & al. [23]; V. TOURNIER & al. [24]; E. Z. L. ZHONG-JOHNSON & al. [25]) directed us towards the optimization and development of facile/accessible recombinant expression system suitable for the production of the PET-degrading enzyme.

Materials and methods

Materials and instrumentation

Tris(hydroxymethyl)aminomethane (TRIS) was purchased from Sigma-Aldrich (USA). The Bradford reagent for protein concentration determinations was purchased from VWR (USA). Technical grade solvents were dried and/or freshly distilled prior to use, while HPLC-grade solvents were purchased from Promochem LGC Standards (Germany). The PET film (product nr. GF25214475-1-EA), bis-(2-hydroxyethyl) terephthalate (BHET) was purchased from Sigma-Aldrich. Terephthalic acid (TPA) was purchased from Alfa Aesar, while mono-(2-hydroxyethyl) terephthalic acid (MHET) was synthesized by previously reported procedure (G. J. PALM & al. [22]). For PCR amplifications Phusion High Fidelity DNA Polymerase (2 U/μL) from Thermo Fisher Scientific was used and a 96-well Eppendorf Mastercycler ProS equipment. Plasmid extraction was performed using GenElute Plasmid Miniprep Kit (Sigma-Aldrich), while the DNA isolation from agarose gel was accomplished using QIAquick Gel Extraction Kit (Qiagen). The T4 DNA Ligase was purchased from Jena Bioscience. Desalting steps from the protein purification procedure were performed using an ÄKTA purifier FPLC (GE Healthcare/Amersham Biosciences) and HiTrap De-

salting columns (Cytiva). UV-Vis measurements were performed on an Agilent 8453 UV-vis spectrophotometer and/or BioTek Epoch 2 microplate reader, using 96-well UV-Microtiter microplates. Enzymatic PET-hydrolysis reactions were carried out in an Eppendorf ThermoMixer C, while HPLC analysis of the reaction samples was conducted on Agilent 1200 instrument. The melting curves of the recombinant proteins were measured using a Bio-Rad CFX 96 Real-Time System and SYPRO Orange Protein Gel Stain (Invitrogen).

Molecular cloning

Cloning the synthetic full-length *ispetase* gene into pET-15b and pET-21a(+) vectors

The codon-optimized synthetic gene encoding the *Is*-PETase, designed with NcoI, NdeI and XhoI restriction sites (**Table S1**), was synthesized by Invitrogen and provided in pMA cloning vector. For subcloning into pET-21a(+) expression vector with a C-terminal His6-tag, the synthetic gene was PCR-amplified without the Stop codon, while for subcloning into pET-15b restriction digestion was employed (the targeted and obtained constructs are presented in **Tables S2**). Accordingly, the amplified gene or the pMA vector harbouring the synthetic gene and empty pET-21a(+) or pET-15b expression vector, respectively, were digested with NdeI and XhoI restriction enzymes for 2 h at 37 °C. The obtained DNA fragments were separated via agarose gel electrophoresis, the DNA bands corresponding to the insert and the recipient plasmid backbone being extracted from the gel and purified. The ligation of the purified DNA fragments was performed for 1 h at 22 °C using T4 DNA ligase, followed by transformation into *E. coli* TOP10 competent cells. The obtained colonies were screened for their insert-content using colony PCR. The plasmid DNA of positive colony/colonies was extracted, and further restriction digestion confirmed the presence of insert gene (**Fig. S1**). The final construct was transformed into different expression hosts (e.g. *E. coli* BL21-Gold (DE3), Rosetta (DE3) pLysS, ArcticExpress (DE3), Rosetta-gami B (DE3)) via heat shock/electroporation for further expression.

Molecular cloning of truncated *Is*PETase (28-290) gene into pET-21a(+) and pET-15b vectors

The first 81 nucleotides corresponding to the signal peptide from the *Is*PETase sequence (residues 1-27) were removed by PCR-amplification using as template DNA the full-length *Is*PETase encoding synthetic gene and the correspondingly designed primers from **Table S3**. The PCR protocol consisted of initial denaturation at 98 °C for 30 s, followed by 30 amplification cycles, each of them involving denaturation at 98 °C for 10 s, annealing at 57 °C for 30 s and extension at 72 °C for 30 s; followed by a final extension step at 72 °C for 10 minutes. The cloning of the truncated *ispetase* gene into pET-21a(+) expression vector was performed using the procedure described for the full-length gene.

For the subcloning of the truncated gene into pET-15b vector the optimized synthetic gene (see *section 2.2.3*) was similarly amplified via PCR using the primers (**Table S6)** allowing Stop codon reinsertion at the 3'-end of the gene. The employed PCR protocol included initial denaturation at 98 °C for 30 s, followed by 30 amplification cycles, each of them consisting of denaturation at 98 °C for 10 s, annealing at 57 °C for 30 s and extension at 72 °C for 30 s; followed by a final extension step at 72 °C for 10 minutes. The cloning of the optimized *ispetase(28-290)* variant into pET-21a(+) expression vector was performed using the procedure described for full-length gene.

Site-directed mutagenesis for sequence optimization

To remove additional ORFs from the codon-optimized synthetic gene encoding *Is*PETase, site-directed mutagenesis was performed using megaprimers (**Table S4**). The PCR protocol consisted of initial denaturation at 98 °C for 30 s, followed by 5 megaprimer amplification cycles (denaturation at 98 °C for 10 s, annealing at 68 °C for 30 s, extension at 72 °C for 2 minutes), followed by 25 cycles for plasmid amplification (denaturation at 98 °C for 30 s and extension at 72 °C for 4 minutes) and a final extension step at 72 °C for 10 minutes. The PCR reaction products were digested with DpnI restriction enzyme at 37 °C for 1 h to remove the DNA template. 5 μL from the digested product was transformed into *E. coli* XL1-Blue chemically competent cells via heat shock. The plasmids isolated from the bacterial colonies were sequenced (Biomi Ltd., Gödöllő) in order to confirm the presence of the mutations.

Transformations into different *E. coli* hosts

The plasmids (pET-21a(+) or pET-15b) harbouring the gene encoding the full-length or truncated *Is*PETase(28-290) were transformed into *E. coli* Rosetta (DE3) pLysS chemically competent cells via heat shock and into *E. coli* BL21-Gold (DE3) electrocompetent cells by electroporation. The plasmids (pET-21a(+) or pET-15b) harbouring the gene encoding the truncated *Is*PETase(28-290) were transformed into *E. coli* ArcticExpress (DE3) host cells via heat shock following the recommendation from the producer. The plasmids (pET-21a(+) or pET-15b) harbouring the improved variant of the gene encoding for truncated *Is*PETase(28-290) were transformed into *E. coli* Rosetta-gami B (DE3) cells via heat shock, following the producer's guidelines.

Protein expression and isolation

Expression and isolation using *E. coli* Rosetta (DE3) pLysS host cells

The recombinant *E. coli* strains harbouring the different *Is*PETase encoding plasmid constructs were grown overnight at 37 °C, in 5 mL Luria-Bertani (LB) medium supplemented with carbenicillin and chloramphenicol. Then, 4 x 0.5 L LB medium was inoculated with 2% (v/v) of the prepared overnight culture and incubated at 37 °C, 220 rpm until OD_{600} = 0.6–0.7 was reached, at which point induction with 0.5 mM (or 1, 1.5 mM) of IPTG was performed, followed by overnight incubation at 20 °C (or, 18, 16 °C), at 180 rpm (or 160 rpm). The cells were harvested by centrifugation at 3000 x *g* for 25 min at 4 °C, followed by resuspension of the cell pellet in lysis buffer (20 mM Tris.HCl, 100 mM NaCl, pH 7.0) and cell disruption by sonication. The cell debris was discarded by centrifugation at 10000 x *g* for 25 min at 4 °C and the *Is*PETase was purified from the cytosolic fraction by gravitational Ni-NTA affinity chromatography. After washing with low salt buffer (50 mM HEPES, 30 mM KCl, pH 7.5) and high salt buffer (50 mM HEPES, 300 mM KCl, pH 7.5), the non-specifically bound proteins were removed with 25 mM imidazole containing buffer (20 mM Tris.HCl, 100 mM NaCl, pH 7.0), followed by the elution of His-tagged proteins with 300 mM imidazole (20 mM Tris.HCl, 100 mM NaCl, pH 7.0). The degree of protein expression and the purity of the obtained fraction was investigated by sodium dodecyl sulphate-polyacrylamide gel electrophoresis (SDS-PAGE) (**Fig. S2, Fig. S3**) and/or Western blot using Mouse anti-His antibody and Rabbit anti-mouse secondary antibody (Invitrogen).

Expression and isolation using *E. coli* BL21 Gold (DE3) host cells

The cell culture preparations for the recombinant *E. coli* BL21-Gold (DE3) strains harbouring the different *Is*PETase encoding plasmid constructs were performed under similar conditions as described in *section 2.4.1*, while the protein isolation protocol via Ni-NTA chromatography followed the previously reported procedures (H. F. SON & al. (2020) [9]; H. F. SON & al. (2019) [21). The eluted protein fraction was subjected to desalting via FPLC, using HiTrap Desalting columns (with Sephadex G-25 resin) and Tris-buffer (20 mM Tris.HCl, 300 mM NaCl, pH 8.0) as mobile phase. The degree of protein expression and the purity of the obtained fraction was investigated by SDS-PAGE (**Fig. S11**), while the protein concentration was determined spectrophotometrically via Bradford method.

Expression and isolation using *E. coli* ArcticExpress (DE3) as host

In case of pET-21a(+) construct containing the improved gene encoding the truncated *Is*PETase, the effect of different cell growth conditions on the protein expression level has been determined in a multi-factorial experiment (**Table S5**). Accordingly, in each case 0.5 L LB medium was inoculated with 2% (v/v) overnight culture and the cells were cultivated at 37 °C, 200 rpm until OD_{600} of 0.6–0.7 followed by induction with different IPTG concentrations (**Table S5**) and overnight incubation at 16 °C or 20 °C and 200 rpm. The cells were harvested by centrifugation at 13000 x *g* for 10 min at 4 °C and suspended in Tris buffer (20 mM Tris.HCl, 100 mM NaCl, pH 7.0), followed by denaturation with SDS-PAGE sample buffer. In case of investigating the autoinduction system ZYM auto inducible medium (F. W. STUDIER [26]) was employed and cell growth was performed by overnight incubation at 16 °C or 20 °C, at 200 rpm. The degree of protein expression, within the samples taken from the different phases of cell growth, was investigated by SDS-PAGE and Western blot techniques.

Expression and isolation using *E. coli* Rosetta-gami B (DE3) host cells

The expression and isolation of the recombinant protein was accomplished as described in the previously reported procedures (H. F. SON & al. (2020) [9]; H. F. SON & al. (2019) [21]). The desalting step was carried out as described above.

In case of the truncated *Is*PETase(28-290) encoding the improved gene/pET-21a(+) construct a similar multi-factorial experiment was carried out as noted above, excepting that the incubation of the cell culture was performed at 20 °C and 25 °C respectively. The degree of protein expression and the purity of the obtained fraction was investigated by SDS-PAGE (**Fig. S10**) and Western blot technique, while the protein concentration was determined using the Bradford method.

PET-hydrolysis reaction

PET-hydrolysis reactions were performed as previously reported (H. F. SON & al. (2020) [9]; S. JOO & al. [20]; H. F. SON & al. (2019) [21]) with slight modifications, using 10 mg of commercial PET film (Sigma-Aldrich) as substrate. The film was soaked in 1 mL of pH 9.0 glycine/NaOH buffer containing 500 nM of isolated *Is*PETase. The reaction mixture was incubated at 45 °C (and/or 30 °C) for 20 h. Samples of 100 µL were removed from the reaction mixture, and in case of UV-activity assay, were analysed directly, while in case of HPLC activity assessments, the reaction samples were quenched by adding an equal volume of acetonitrile,

vortexed and centrifuged (17000 x *g*, 3 minutes), followed by acidification of the supernatant and filtering through a 0.2 μM nylon membrane.

Activity assessment by HPLC

The employed procedure was similar to previously reported methods (H. F. SON & al. (2020) [9]; S. JOO & al. [20]; H. F. SON & al. (2019) [21]; C. LIU & al. [23]), using an Agilent 1200 HPLC system, equipped with DAAD detector. The samples, retrieved from the biocatalytic PET-hydrolysis reactions, were injected onto a Phenomenex Luna C8(2) column (150x4.6 mm; 5 μm), eluted with a flow rate of 1.0 mL/min at 20 °C using a linear gradient elution of the mobile phase consisting of (A) 0.1% formic acid solution and (B) acetonitrile, with varied composition of 15% (B) to 27.5% (B) over 10 minutes elution time, monitoring the product elution at 240 nm. All experiments were performed in triplicate. TPA, MHET, and BHET (the total TPA) content of the reaction samples, and implicitly the enzyme activity, was determined based on calibration curves using the authentic standard of TPA and BHET (Sigma-Aldrich) and synthesized MHET.

Enzyme activity assessment via UV-Vis spectroscopy

The PET-hydrolysis reaction was analysed using the previously described bulk absorbance method (E. Z. L. ZHONG-JOHNSON & al. [25]). UV-absorbance spectra (**Fig. S12**) were determined for all three PET-hydrolysis products (TPA, MHET and BHET) using their 0.1 mM solutions in glycine/NaOH pH 9.0 buffer. Based on this, 235 nm was selected as wavelength for UV-activity measurements (**Fig. 2B**), since at this wavelength the absorbance of the three compounds show the closest magnitude. Further, the extinction coefficients at 235 nm within the glycine/NaOH pH 9.0 buffer were determined for each hydrolysis product separately, the results resembling the reported values (E. Z. L. ZHONG-JOHNSON & al. [25]). Using the average extinction coefficient, the total product (TPA content) of the samples from the PET-hydrolysis reaction could be determined through A_{235} measurements.

Melting temperature (T_M) assessments

The thermostability measurements were performed using differential scanning fluorimetry (DSF). The protein solutions at a concentration of 5-10 μM were mixed with SYPRO Orange dye and glycine/NaOH (pH 9.0) buffer to a final volume of 50 μL. The 5000x stock of the SYPRO Orange dye solution was diluted to 200x with glycine/NaOH (pH 9.0) buffer, then 5 μL of the diluted colorant was added to each sample. The obtained protein samples were loaded into a white-clear-Hard Shell 96-well PCR plate (Bio-Rad), followed by sealing the plate with optically clear Microseal B sealing tape (Bio-Rad). The melting curve of the samples were then measured using the FAM and ROX channels of a Bio-Rad CFX96 system, with 450-490 and 560-590 excitation and 510-530 and 610-650 emission filters, respectively. The samples were heated on a temperature range from 20 °C to 95 °C, while the melting temperature was determined from the peaks of the first derivatives of the melting curve.

Results and discussion

For the production of recombinant *Is*PETase various plasmid constructs, including the full-length *ispetase* gene encoding 290 amino acids with an additional polyhistidine-tag and different types of *E. coli* as expression host cells have been reported (**Table 1**) (H. P. AUSTIN & al. [10]; E. ERICKSON & al. [31]). On the other hand, in several works (H. F. SON & al. (2020) [9]; S. JOO & al. [20]; H. F. SON & al. (2019) [21]; G. J. PALM & al. [22]; C. LIU & al. [23]; V. TOURNIER & al. [24]; E. Z. L. ZHONG-JOHNSON & al. [25]) the expression of *Is*PETase enzyme was performed from the truncated *ispetase* gene (amino acid residues 28-290), lacking the signal sequence (amino acid residues 1-27) (**Table 1**).

Accordingly, we targeted the expression and purification of both the full-length or truncated *ispetase* genes. The nucleotide sequence of *Is*PETase (Genbank: GAP38373.1) was codon optimized and the synthetic gene (**Table S1**) was used for cloning as full-length or truncated version into pET-15b vector (**Fig. S1**), providing an *N*-terminal His-tag. Expression in different *E. coli* host strains, Rosetta (DE3) pLysS, BL21-Gold (DE3), proved to be unsuccessful, no detectable (SDS-PAGE, Western-blot) *Is*PETase levels being registered. The expression of recombinant *Is*PETase with *N*-terminal His-tag (**Fig. S1**) and protein purification by affinity chromatography revealed low protein yields (~1-2 mg from 1 L culture) and no protein band at the expected size of *Is*PETase (~30.1 kDa for full-length version and ~27.7 kDa for truncated *Is*PETase) (**Fig. S2**). Optimization of the expression parameters, such as testing the effect of different incubation temperatures (20 °C, 18 °C and 16 °C) (**Fig. S3**) and the effect of IPTG concentration (0.1, 0.5 and 1 mM) was also performed, however no expression of *Is*PETase had been observed. The Western blot analysis revealed the presence of His-tagged proteins with molecular weights <25 kDa within the induced cells, suggesting possible proteolysis of the targeted protein, while no protein bands were detected within the fractions resulted from protein purification (**Fig. S4**).

Table 1. Reported recombinant expression systems for the production of *Is*PETase.

Entry	*Is*PETase encoding gene	Expression vector	Affinity tag	Expression host	Enzyme activity	Specific activity (mg_{TPAeq}/h/$mg_{IsPETase}$)	Reference
1	truncated	pET-15b	N-terminal His_6-tag	Rosetta gami-B	8.6 µM TPA_{eq} in 24 h	~0.095	H. F. SON & al. [9, 21]
2	full-length	pET-21b(+)	C-terminal (modified) 5xHis-tag	C41(DE3)	[a]	-	H. P. AUSTIN & al. [10]
3	truncated	pET-30a	not mentioned	BL21 (DE3)	[a]	-	X. MENG & al. [27]
4	truncated	pET-15b	N-terminal His_6-tag	Rosetta gami-B	3 mg/L TPA_{eq} in 18 h	~0.027	S. JOO & al. [20]
5	truncated	pET-21b	C-terminal His_6-tag	ArcticExpress (DE3)	[b]	-	C. LIU & al. [23]
6	truncated (*Trx-*Is*PETase)	pET-28b(+) (pET-32b(+))	C-terminal His_6-tag	Rosetta-gami 2	0.7 (0.9) mg_{TPAeq}/h/$mg_{IsPETase}$	0.7 (0.9)	P. WAGNER-EGEA & al. [28]
7	truncated	pET-21b(+)	C-terminal His_6-tag	*Shuffle* T7	[a]	-	G. J. PALM & al. [22]
8	truncated	pET-21a(+)	C-terminal His_6-tag	T7 Express	[b]	-	E. Z. L. ZHONG-JOHNSON & al. [25]
9	$SP_{LamB.}$ *Is*PETase**	pET-22b(+)	C-terminal His_6-tag	-	~2.5 mg/L/24 h 200 nM	~0.017	H. SEO & al. [29]
11	full length	pET32a (pPICZαA)	not mentioned	BL21 trxB (DE3) (*P. pastoris* X33)	[c]	-	C. CHEN & al. [30]
12	full-length	pET-21b(+)	C-terminal His_6-tag	C41(DE3)	1.2 mM aromatic product in 24 h	~0.28	E. ERICKSON & al. [31]
13	truncated	pET-21b(+)	C-terminal His_6-tag	BL21 (DE3)	10^{-2} mg_{TPAeq}/h/$mg_{IsPETase}$	~0.01	V. TOURNIER & al. [24]

[a] The activity of the *Is*PETase not mentioned in conversional units, [b] only kinetic measurements performed towards napthyl ester polymers, [c] reaction volume (for activity deduction) not stated.

* *ispetase* gene with a thioredoxin fusion domain (Trx) at the N-termini.

** leader sequence replaced with *sec*-dependent maltoporin signal peptide in order to produce extracellularly the *Is*PETase.

Further, the truncated version of the *Is*PETase encoding gene was subcloned into pET-21a(+) using restriction sites NdeI and XhoI (**Fig. S5 and Table S3**), providing a C-terminal His-tag to the recombinant protein, however successful expression of *Is*PETase was not achieved, no protein band at the expected size could be observed by SDS-PAGE and Western-blot analysis (**Fig. S6, Fig. S7**). Additionally, to exclude protein folding issues we tested the expression of the truncated gene in *E. coli* ArcticExpress (DE3) host-cells, derived from BL21-Gold (DE3), featuring chaperonins Cpn60 and Cpn10 that facilitate proper folding also at low temperatures, strain previously being reported as successful host for *Is*PETase production (C. LIU & al. [23]). Since again *Is*PETase production was not detectable (**Fig. S8**), the synthetic gene, codon optimized by Invitrogen, was further optimized via the removal of the secondary open reading frame through site-directed mutagenesis (**Fig. S9**, **Table S4**), maintaining the encoded *Is*PETase sequence unaltered. The obtained plasmid harbouring the truncated version of the improved *Is*PETase in pET-21a(+), was transformed into *E. coli* ArcticExpress (DE3) and Rosetta-gami B (DE3) cells, the later also known to enhance the expression of genes with rare codons and also to facilitate proper disulphide bond formation within the protein-folding process (H. F. SON & al. (2020) [9]; S. JOO & al. [20]; H. F. SON & al. (2019) [21]; P. WAGNER-EGEA & al. [28]). Within these two hosts the production of *Is*PETase was attempted, varying the expression conditions (**Table S5**), such as medium type, induction and cell-growth temperature. Despite the multi-factorial experimental set-up, the expression of the desired protein was found to be unsuccessful.

In the final successful attempt, the use of an *N*-terminal His-tag for the truncated, improved gene sequence was considered. Accordingly, we subcloned the truncated, overlapping ORF-lacking *ispetase* gene into the pET-15b vector, then transformed the construct into both *E. coli*

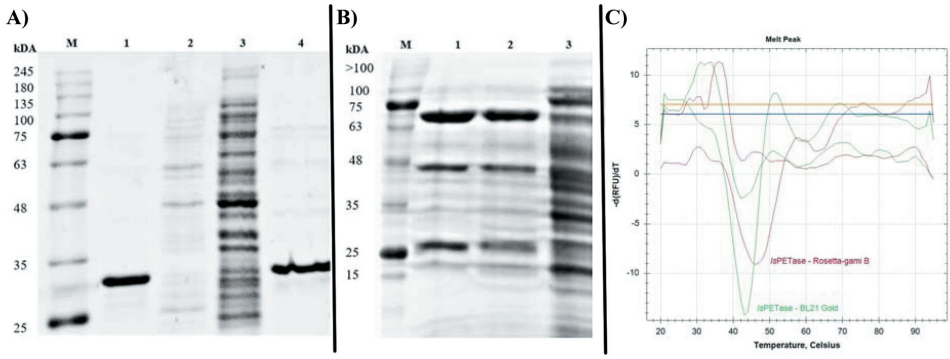

Figure 1. SDS-PAGE analysis of the isolation of mutant *Is*PETase(28-290)-pET-15b using as host *E. coli* **A)** Rosetta-gami B(DE3) cells (M-protein ladder, 1-eluted fraction (300 mM imidazole), 2-washing with 30 mM imidazole, 3-second flow-through, 4-eluted protein after desalting) and **B)** BL21 Gold (DE3) cells (M-protein ladder, 1-eluted protein after desalting, 2- second flow-through, 3-washing with 30 mM imidazole). **C)** Melting temperature measurement of the obtained *Is*PETase enzyme via differential scanning fluorimetry (DSF) (by plotting the negative first derivative of the fluorescence vs the temperature).

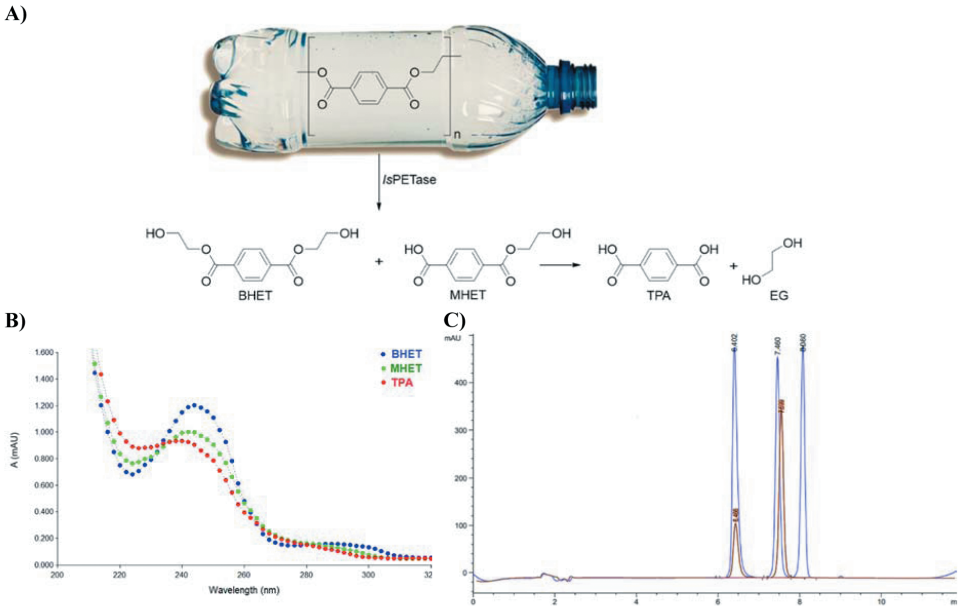

Figure 2. PET degrading activity of the produced recombinant *Is*PETase**. A)** Reaction scheme for the enzymatic PET film degradation. **B)** Overlay UV absorbance spectra of terephthalic acid (TPA), mono-(2-hydroxyethyl) terephthalic acid (MHET) and bis-(2-hydroxyethyl) terephthalate (BHET). **C)** Overlay of the HPLC chromatograms of *i*) the separation of TPA (1st peak), MHET (2nd peak) and BHET (3rd peak) during the measurements within standard curve assessment (blue) and *ii)* of sample from the enzymatic PET hydrolysis reaction (after 24-hour reaction time) (orange).

BL21-Gold (DE3) and Rosetta-gami B (DE3) expression hosts. In both cases, the SDS-PAGE analysis revealed the expression of a ~29 kDa protein, present also within the fraction eluted from the affinity chromatography (**Fig. 1A, Fig. 1B, see also Fig. S10 and Fig. S11**). Interestingly, using Rosetta-gami B as host *Is*PETase have been obtained in high purity (>95% - estimated from SDS-PAGE – **Fig. 1A**) and titer yields of (2.5 mg/L ferment), while in case of expression in *E. coli* BL21-Gold (DE3) host cells significantly lower expression yields (1.5 mg/L ferment)

and lower protein purity have been obtained (**Fig. 1B**). These results strengthen that the formation of the two disulphide-bonds Cys203-Cys239 and Cys289-C273 found within the crystal structures of *Is*PETase monomers (PDB ID: 5XJH) are essential within protein expression in *E. coli* host. Since Rosetta-gami B host cells with mutations in both the thioredoxin reductase (*trxB*) and glutathione reductase (*gor*) genes, enhanced disulphide bond formation in the *E. coli* cytoplasm, it also promoted the proper folding and expression of *Is*PETase. Notable, that in our case the same truncated gene version cloned with a C-terminal His6-tag in the pET-21a(+) vector repeatedly resulted in unsuccessful protein expression even in Rosetta-gami B, despite successful expression of similar C-terminal His6-tagged *Is*PETase encoding truncated genes in pET-21a(+) constructs being reported, *albeit* in other, disulphide bridge formation favouring, T7 Shuffle or T7 express *E. coli* hosts (G. J. PALM & al. [22]; E. Z. L. ZHONG-JOHNSON & al. [25]). The proximity of the C-terminal disulphide-bridge forming C289, and the disulphide bridge forming capability of Rosetta-gami B strains seems of high importance for protein folding/stability, reflected in the more facile expression of *N*-terminal tagged *Is*PETase.

Our results underline the importance of the selection/optimization of the cloning strategy, revealing several non-reported issues hindering the recombinant expression of *Is*-PETase. Apparently, the reported data suggest that PETase activity is not affected by the different N- or C-terminal positioning of the His-tag, however their *in vivo* folding process might be differently affected in the employed *E. coli* hosts, improperly folded *Is*PETase being exposed to protease degradation, as supported by our results.

The thermal stability assessment of the purified *Is*PETase revealed a melting temperature of 46.2°C, (**Fig. 1C**), in agreement with reported values (H. F. SON & al. (2020) [9]; H. P. AUSTIN & al. [10]; S. JOO & al. [20]; H. F. SON & al. (2019) [21]; C. LIU & al. [23]; E. Z. L. ZHONG-JOHNSON & al. [25]). The activity of the obtained *Is*PETase was investigated within the hydrolysis reaction of PET film (**Fig. 2**) using previously reported HPLC (H. F. SON & al. (2020) [9]; S. JOO & al. [20]; H. F. SON & al. (2019) [21]; V. TOURNIER & al. [24]) and UV-spectroscopy (E. Z. L. ZHONG-JOHNSON & al. [25]) methods.

During the analytical scale PET film degradation, we monitored the formation of the three possible products with terephthalic acid (TPA) content, bis-(2-hydroxyethyl) terephthalate (BHET), mono-(2-hydroxyethyl) terephthalate (MHET) and TPA (**Fig. 2A**), from which the global TPA quantity produced upon PET-hydrolysis could be obtained. During the UV-spectroscopy based PETase-activity measurements the molar absorptivity for each reaction product, BHET, MHET, TPA was determined (**Fig. S12**), using, as previously reported (E. Z. L. ZHONG-JOHNSON & al. [25]), the medium molar absorptivity, for products concentration assessments from UV-absorbance measurements at 235 nm. Further, the PETase activity measurements were also performed by employing HPLC procedures (H. F. SON & al. (2020) [9]; S. JOO & al. [20]; H. F. SON & al. (2019) [21]; V. TOURNIER & al. [24]), that upon adaptation provided baseline separation of the three TPA unit containing PET-hydrolysis product, TPA, MHET, BHET (**Fig. 2C**), while calibration using their authentic standard solutions provided quantification of the total TPA content of the samples extracted from enzymatic reactions (**Fig. 2C**).

Accordingly, the PET-hydrolysing activity of the produced *Is*PETase at 45 °C was 0.08 mg TPA produced / mg enzyme / 1 h reaction time with the UV-assay, while HPLC measurements revealed activity of 0.02 mg TPA produced / mg enzyme / 1 h reaction time, both values being in accordance with reported activity values (H. F. SON & al. (2020) [9]; S. JOO & al. [20]; H. F. SON & al. (2019) [21]; V. TOURNIER & al. [24]; H. SEO & al. [29]) and support that the optimized expression system is suitable for the facile production of *Is*PETase.

Conclusions

Within the present study we targeted the recombinant expression of the leading PET-degrading enzyme, *Is*PETase. Employing several reported expression systems, providing different N- or C-terminal affinity tags and various *E. coli* expression hosts, we registered unsuccessful *Is*PETase expressions. Construct and expression host optimizations revealed that the N-terminal His-tag and Rosetta-gami B expression host provided *Is*PETase in high yield and purity. The thermal denaturation profile and PET-hydrolysing activity of the isolated *Is*PETase was in agreement with reported data, supporting its proper fold. The results, while revealing several non-reported issues hindering the recombinant expression of *Is*PETase, suggest that the *in vivo* folding process of *Is*PETase might be differently affected among the different *E. coli* hosts. The revealed issues/solutions underline the importance of the selection/optimization of the cloning strategy for the successful recombinant expression of the *Is*PETase.

Conflicts of interest

The authors declare no conflicts of interest.

Acknowledgements

I. H. thanks the STAR-Institute of the Babeș-Bolyai University for the provided student-research fellowship and K. B. thanks for the support provided by the Collegium Talentum Programme of Hungary.

References

1. W. Courtene-Jones, B. Quinn, S. F Gary, A. O. M. Mogg, B. E Narayanaswamy, Microplastic pollution identified in deep-sea water and ingested by benthic invertebrates in the Rockall Trough, North Atlantic Ocean, Environ. Pollut., 231(1), 271, 280 (2017).
2. L. Nizzetto, M. Futter, S. Langaas, Are Agricultural Soils Dumps for Microplastics of Urban Origin?, Environ. Sci. Technol., 50(20), 10777, 10779 (2016).
3. C. E. Enyoh, A. W. Verla, E. N. Verla, F. C. Ibe, C. E. Amaobi, Airborne microplastics: a review study on method for analysis, occurrence, movement and risks, Environ. Monit. Assess., 191(668), 1, 17 (2019).
4. C. L. Waller, H. J. Griffiths, C. M. Waluda, S. E.Thorpe, I. Loaiza, B. Moreno, C. O.Pacherres, K. A. Hughes, Microplastics in the Antarctic marine system: An emerging area of research, Sci. Total Environ., 598, 220, 227 (2017).
5. R. H. Waring, R. M. Harris, S. C. Mitchell, Plastic contamination of the food chain: A threat to human health?, Maturitas, 115, 64, 68 (2018).
6. E. S. Gruber, V. Stadlbauer, V. Pichler, K. Resch-Fauster, A. Todorovic, T. C. Meisel, S. Trawoeger, O. Hollóczki, S. D. Turner, W. Wadsak, A. D. Vethaak, L. Kenner, To Waste or Not to Waste: Questioning Potential Health Risks of Micro- and Nanoplastics with a Focus on Their Ingestion and Potential Carcinogenicity, Expos. Health (2022).
7. K. Ragaerta, L. Delva, K. Van Geem, Mechanical and chemical recycling of solid plastic waste, Waste Manage., 69, 24, 58 (2017).
8. R. J. Müller, H. Schrader, J. Profe, K. Dresler, W.-D. Deckwer, Enzymatic Degradation of Poly(ethylene terephthalate): Rapid Hydrolyse using a Hydrolase from T. fusca, Macromol. Rapid. Commun., 26(17), 1400, 1405 (2005).
9. H. F. Son, S. Joo, H. Seo, H.-Y. Sagong, S. H. Lee, H. Hong, K.-J. Kim, Structural bioinformatics-based protein engineering of thermo-stable PETase from Ideonella sakaiensis, Enzyme Microb. Tech., 141, 109656 (2020).
10. H. P. Austin, M. D. Allen, B. S. Donohoe, N. A. Rorrer, F. L. Kearns, R. L. Silveira, B. C. Pollard, G. Dominick, R. Duman, K. E. Omari, V. Mykhaylyk, A. Wagner, W. E. Michener, A. Amore, M. S. Skaf, M. F. Crowley, A. W. Thorne, C. W. Johnson, H. L. Woodcock, J. E. McGeehan, G. T. Beckham, Characterization and engineering of a plastic-degrading aromatic polyesterase, PNAS, 115(19), E4350, E4357 (2018).
11. Y. Ma, M. Yao, B. Li, M. Ding, B. He, S. Chen, X. Zhou, Y. Yuan, Enhanced Poly(ethylene terephthalate) Hydrolase Activity by Protein Engineering, Engineering, 4(6), 888, 893 (2018).
12. H. Y. Sagong, H. Seo, T. Kim, H. F. Son, S. Joo, S. H. Lee, S. Kim, J.-S. Woo, S. Y. Hwang, K.-J. Kim, Decomposition of the PET Film by MHETase Using Exo-PETase Function, ACS Catal., 10(8), 4805, 4812 (2020).
13. R. Wei, D. Breite, C. Song, D. Gräsing, T. Ploss, P. Hille, R. Schwerdtfeger, J. Matysik, A. Schulze, W. Zimmermann, Biocatalytic Degradation Efficiency of Postconsumer Polyethylene Terephthalate Packaging Determined by Their Polymer Microstructures, Adv. Sci., 6(14), 1900491 (2019).
14. F. Kawai, T. Kawabata, M. Oda, Current knowledge on enzymatic PET degradation and its possible application to waste stream management and other fields, Appl. Microbiol. Biotechnol., 103, 4253, 4268 (2019).
15. F. Kawai, T. Kawabata, M. Oda, Current State and Perspectives Related to the Polyethylene Terephthalate Hydrolases Available for Biorecycling, ACS Sustain. Chem. Eng., 8(24), 8894, 8908 (2020).
16. a) T. Brueckner, A. Eberl, S. Heumann, M. Rabe, G. M. Guebitz, Enzymatic and chemical hydrolysis of poly(ethylene terephthalate) fabrics, J. Polym. Sci. Pat. A: Polym. Chem., 46(19), 6435, 6443 (2008). b) E. H. Acero, D. Ribitsch, G. Steinkellner, K. Gruber, K. Greimel, I. Eiteljoerg, E. Trotscha, R. Wei, W. Zimmermann, M. Zinn, A. Cavaco-Paulo, G. Freddi, H. Schwab, G. Guebitz, Enzymatic surface hydrolysis of PET: effect of structural diversity on kinetic properties of cutinases from Thermobifida, Macromolecules, 44(12), 4632, 4640 (2011). c) F. Kawai, T. Kawase, T. Shiono, H. Urakawa, S. Sukigara, C. Tu, M. Yamamoto, Enzymatic hydrophilization of polyester fabrics using a recombinant cutinase Cut190 and their surface characterization, J. Fiber. Sci. Technol., 73(1), 8, 18 (2017).
17. M. A. M. E. Vertommen, V. A. Nierstrasz, M. van der Veer, M. M. C. G. Warmoeskerken, Enzymatic surface modification of poly(ethyleneterephthalate), J. Biotechnol., 120(4), 376, 386 (2006).
18. I. Taniguchi, S. Yoshida, K. Hiraga, K. Miyamoto, Y. Kimura, K. Oda, Biodegradation of PET: Current Status and Application Aspects, ACS Catal., 9(5), 4089, 4105 (2019).

19. S. Yoshida, K. Hiraga, T. Takehana, I. Taniguchi, H. Yamaji, Y. Maeda, K. Toyohara, K. Miyamoto, Y. Kimura, K. Oda, A bacterium that degrades and assimilates poly(ethylene terephthalate), Science, 351(6278), 1196, 1199 (2016).
20. S. Joo, I. J. Cho, H. Seo, H. F. Son, H.-Y. Sagong, T. J. Shin, S. Y. Choi, S. Y. Lee, K.-J. Kim, Structural insight into molecular mechanism of poly(ethylene terephthalate) degradation, Nat. Commun., 9, 382 (2018).
21. H. F. Son, I. J. Cho, S. Joo, H. Seo, H.-Y. Sagong, S. Y. Choi, S. Y. Lee, K.-J. Kim, Rational Protein Engineering of Thermo-Stable PETase from Ideonella sakaiensis for Highly Efficient PET Degradation, ACS Catal., 9(4), 3519, 3526 (2019).
22. G. J. Palm, L. Reisky, D. Böttcher, H. Müller, E. A. P. Michels, M. C. Walczak, L. Berndt, M. S. Weiss, U. T. Bornscheuer, G. Weber, Structure of the plastic-degrading Ideonella sakaiensis MHETase bound to a substrate, Nat. Commun., 10, 1717 (2019).
23. C. Liu, C. Shi, S. Zhu, R. Wei, C.-C. Yin, Structural and functional characterization of polyethylene terephthalate hydrolase from Ideonella sakaiensis, Biochem. Bioph. Res. Co., 508(1), 289, 294 (2019).
24. V. Tournier, C. M. Topham, A. Gilles, B. David, C. Folgoas, E. Moya-Leclair, E. Kamionka, M.-L. Desrousseaux, H. Texier, S. Gavalda, M. Cot, E. Guémard, M. Dalibey, J. Nomme, G. Cioci, S. Barbe, M. Chateau, I. André, S. Duquesne, A. Marty, An engineered PET depolymerase to break down and recycle plastic bottles, Nature, 580, 216, 219 (2020).
25. E. Z. L. Zhong-Johnson, C. A. Voigt, A. J. Sinskey, An absorbance method for analysis of enzymatic degradation kinetics of poly(ethylene terephthalate) flms, Sci. Rep., 11, 928 (2021).
26. F. W. Studier, Protein production by auto-induction in high density shaking cultures, Protein Expr. Purif., 41(1), 207, 234 (2005).
27. X. Meng, L. Yang, H. Liu, Q. Li, G. Xu, Y. Zhang, F. Guan, Y. Zhang, W. Zhang, N. Wu, J. Tian, Protein engineering of stable IsPETase for PET plastic degradation by Premuse, Int. J. Biol. Macromol., 180, 667, 676 (2021).
28. P. Wagner-Egea, V. Tosi, P. Wang, C. Grey, B. Zhang, J. A. Linares-Pastén, Assessment of IsPETase-Assisted Depolymerization of Terephthalate Aromatic Polyesters and the Effect of the Thioredoxin Fusion Domain, Appl. Sci., 11(18), 8315 (2021).
29. H. Seo, S. Kim, H. F. Son, H.-Y. Sagong, S. Joo, K.-J. Kim, Production of extracellular PETase from Ideonella sakaiensis using secdependent signal peptides in E. coli, Biochem. Biophys. Res. Commun., 508(1), 250, 255 (2019).
30. C.-C. Chen, X. Han, X. Li, P. Jiang, D. Niu, L. Ma, W. Liu, S. Li, Y. Qu, H. Hu, J. Min, Y. Yang, L. Zhang, W. Zeng, J.-W. Huang, L. Dai, R.-T. Guo, General features to enhance enzymatic activity of poly(ethylene terephthalate) hydrolysis, Nat. Catal., 4, 425, 430 (2021).
31. E. Erickson, T. J. Shakespeare, F. Bratti, B. L. Buss, R. Graham, M. A. Hawkins, G. König, W. E. Michener, J. Miscall, K. J. Ramirez, N. A. Rorrer, M. Zahn, A. R. Pickford, J. E. McGeehan, G. T. Beckham, Comparative Performance of PETase as a Function of Reaction Conditions, Substrate Properties, and Product Accumulation, ChemSusChem., 15(1), e202101932 (2022).